



Testing and Prediction of Flare Emissions from Transient Ignition



Joseph D Smith^{1*}, Hayder A Al Hameedi¹, Robert Jackson² and Ahti Suo Antilla²

¹Chemical and Biochemical Engineering Department, Missouri University of Science and Technology, USA

²Elevated Analytics Inc., USA

***Corresponding author:** Joseph D Smith, Chemical and Biochemical Engineering Department, Missouri University of Science and Technology, Rolla, MO, USA, 65409

Submission: April 24, 2018; **Published:** May 09, 2018

Abstract

Computational fluid dynamics (CFD) was used to simulate multi tip flare system with different operating conditions during ignition time. Single tip and three tips flare systems were simulated and verified against experimental test to get CFD combustion model that required for multi tip flare system. Natural gas, propane, propylene, ethylene and xylene were used as flaring gases in simulated tests of single and three tips flare under an open environment that carried out at the Zeeco facility in Tulsa, OK. This study aimed to predict the soot formation and heat radiation from full multi tip flare field by using CFD modelling with verified combustion model and large eddies simulation (LES) turbulence model with a reduced four step combustion mechanism. The results showed that the multi tip flare system performance can be predicted by using C3d tool.

Keywords: CFD; Multi tip flare; Radiation; Emissions; Combustion; Flare performance; Flare regulations

Introduction

Flares are the most important safety equipment during upset or sudden shutdown events in the chemical and petrochemical plants. They are combusting relief and unusable flammable gases in an open atmosphere to prevent tragic events in the whole system. Also, they used to prevent the atmospheric pollution with different contaminants by converting them to CO₂ and water. Many steps have been taken by different countries towards reducing the amount of gas flaring around the world. However, the global trend of gas flaring is increased each year due to increasing of global oil and gas production where the estimated amount of gas flared in 2012 was 145 billion cubic meters and in 2016 was 149 billion cubic meters [1,2]. Additionally, regulations for flaring process operation and design such EPA 40 CFR 60.18, and API 521 have been established to ensure high flare performance [3,4]. However, in the flaring process, ignition can be delayed for unlit flares or extinguished pilot flame flares and hence unburned hydrocarbons and black carbon (BC) release to the atmosphere.

During the flare ignition process, the hydrocarbon gas is fed through a stack into the atmosphere where it is ignited using an external energy source. This phenomenon is clearly seen by the incomplete combustion that occurs moments after flare ignition where BC emissions form during the flare ignition process. This transient is caused by the inefficient mixing of flare gas and air during first 10-30 seconds of flare operation. Therefore, large

amount of BC release to the ambient air. On the other hand, heat is released by combustion reaction of vent gas with oxygen during flaring process.

Black carbon has a negative influence on the climate and human health. For example, when black carbon deposits on reflective object surfaces, it could darken these surfaces and cause a decrease in albedo (percentage of reflected solar radiation from the object to space), e.g. snow, ice, and white surfaces. By absorbing solar radiation, BC causes melting of snow and ice. Also, BC can influence the cloud dynamics and properties by absorption radiation from the atmosphere. Moreover, BC can affect the human health by causing respiratory illnesses, cancer, and congenital defect [5]. On the other hand, part of the heat that release from combustion reaction radiated to the surrounding facilities and objects. Therefore, flares should be far enough or have suitable distance from other objects to avoid the heat radiation effect on the workers and other equipment. Consequently, estimation of heat radiation rate from flaring practice is essential in designing task of flares.

Many studies on measuring and estimation of BC emission from flaring process have been carried out [6-12]. Most of these studies reported that the BC emission is increasing with decreasing the flare combustion efficiency. McEwen J et al. [8] measured the quantitative emission of soot in lab scale flares of 12.7-76.2mm inner diameters with jet velocity 0.1-2.2m/sec, four and six component methane-based fuel mixtures. They found an empirical relationship between

heating value (HV, MJ/m³) of flare vent gas and the soot emission factor, SEF (kg of soot/103m³ fuel), as shown in equation (1).

$$\text{SEF} = 0.0578 \cdot \text{HV} - 2.09 \quad (1)$$

Wang et al. [12] suggested a new reaction mechanism with 50 components to predict soot emission by predicting important soot precursor species such as C₂H₂, C₂H₄ and C₆H₆. They showed that CFD simulation of an air assisted flare with this mechanism better predicted soot emission from the flare. Several investigations have been done to study the thermal radiation emissions [13-18] from flares. Smith et al. [16] evaluated the effect of the flaring operation of multiple flares on the neighbouring flaring system fields at the maximum flow rates by using CFD technique. Smith et al. [17] studies the effects of the flare plume from multi point ground flares on surrounding facilities and workers at the maximum flow rates using LES based CFD simulations. Recently, a new modelling approach to predict heat radiation from gas flaring has been introduced by Miller [18]. However, this model has been developed for H₂ and syngas flaring.

Materials and Methods

Testing

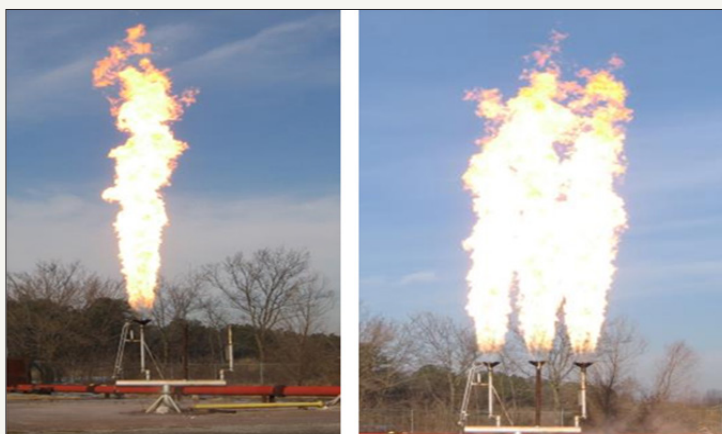


Figure 1: General view for the single and three tips flare [14].



Figure 2: Multi arm flare burner tip (courtesy of Zeeco, Inc.).

One set up for the experimental tests has been used in this study to measure soot emission and heat radiation emissions from single tip and three tips flare. A view of experimental rig is shown in Figure 1. The purpose of these experiments was to provide the required data for validation with the CFD combustion model that is needed later for the simulation of full multi tips flare system.

Analytical quantification of an elevated multi-point flare (MPF) operating at full-rate is very difficult. These difficulties are due to the large size of the combined flame from multiple burner tips operating in the multi-point flare and the associated high radiation flux from a flare operating high above the ground. Due to the large plume emitted from a MTF with the associated high heat radiation, emission measurements are also very difficult to perform. The API 521 flaring guidelines includes design criteria for a flaring system but focus on utility flares and assisted flares with little consideration for MPF flares. Therefore, additional performance metrics are needed for MTF design and performance [13]. To the author's knowledge, none of these studies that mentioned above regarding soot emission estimated BC emissions from flares during the flare ignition process. Therefore, the objective of this study was to estimate the amount of BC released during the ignition time of flare system annually. Also, the thermal radiation to the surrounding, and the formed soot estimation for MTF systems have been simulated using CFD technique.

Different flare burner tips are used in flaring system such as pipe burner and multi arm burner to handle large amount of waste gases especially in the oil and gas production field. The advantages of using multi-arm burner are to improve the local turbulence and mixing of flaring gas with air. Also, these burners minimize the thermal radiation levels because of its resistance to wind deviation.

They are fabricated from 310 stainless steel casting materials via investment casting to increase the operating life of the burner. To get a safe and reliable operation of these burners, they are tested against pressure in the manufacturing factory. A view of multi arm burner is shown in Figure 2. The single flare tip was consisted of main horizontal tube join to another vertical tube with one multi arm burner while three tip flare was included one main horizontal tube connected to three vertical tubes with one multi arm burner at the end of each vertical tube as shown in Figure 2.

The experimental tests were carried out at Zeeco Inc. facility in Tulsa, OK, using wide range of gases such as methane, propane, propylene ethylene and xylene. Thermal radiation measurements were performed in two different locations for the single and there tip flares; the first one lies 5 meters far from the flare tip and the

second location lies 20 meters from the flare tip. Two circumstances for cross wind velocity have been considered where one of those velocities is zero. The other velocity for the cross wind was chosen to be 3 meters per hour.

Results of testing: The effect of the cross-wind velocity for single tip flare tip with propane as a vent gas is presented in Figure 3. When there was no wind, then the shape of the flame above the flare tip was elongated and similar to the pencil shape. As shown in Figure 3, the wind speed effects flame shape and causes the flame to be bent. Also, the wind speed reduce the flame temperture and hence the thermal radiation decreases. When the cross wind velocity 8 to 10 mile per hour (mph) , the flame titled towards downside of wind with an angle of 8° and the height of flame was 10.5 meters where the height reduction around 30 percent as shown in Figure 3

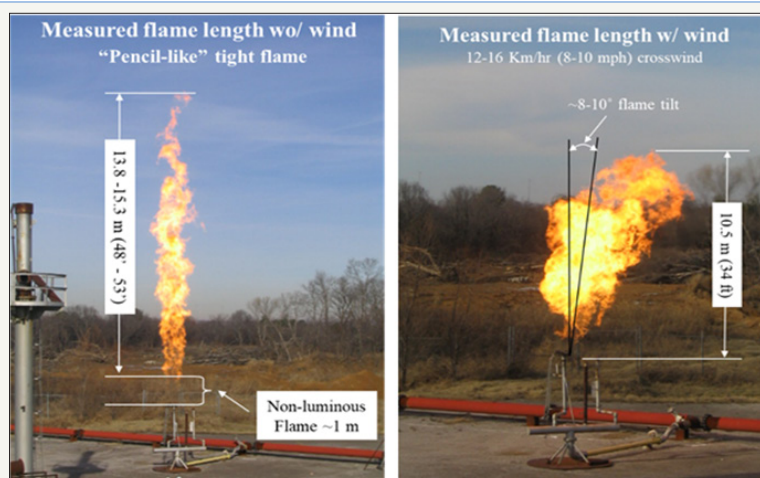


Figure 3: Wind effects on the flame shape of single flare tip with propane flow rate: measured at 1.4 in-wc @ 57 °F across orifice plate (7.3 psig tip pressure on 18 inch pipe) [13].

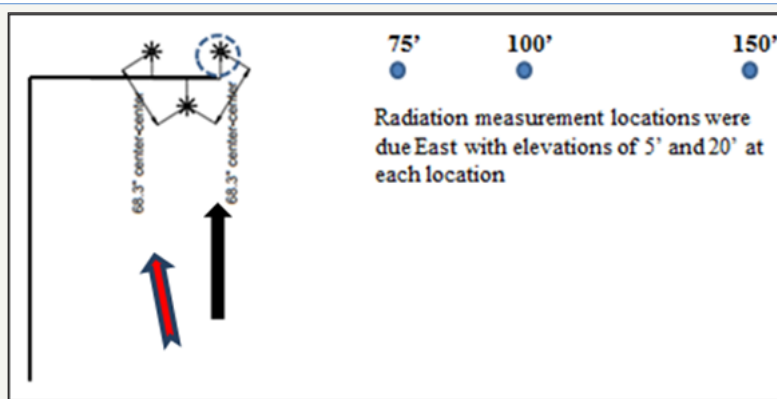


Figure 4: Setup for radiation measurements from single tip flare.

Table 1: Radiation heat flux measurement for single tip burner.

Wind Speed	Position (m)	Radiation Heat Flux (W/m ²)	Radiation Heat Flux (W/m ²)
		Distance from Grade = 5ft	Distance from Grade = 20ft
6-12mph wind speed	22.86 (75 ft)	540.22	648.26
	30.48 (100 ft)	324.13	324.13
	45.72 (150 ft)	108.04	108.04

6mph wind speed	22.86 (75 ft)	540.22	648.26
	30.48 (100 ft)	324.13	324.13
	45.72 (150 ft)	108.04	108.04

The test setup for heat radiation from single tip is displayed in Figure 4. For thermal radiation measurements a 6-12mph wind speed blowing mostly from south to the north with an angle of 169° were implanted during single tip test with propylene fuel as shown in Figure 4. These measurements were taken in three different positions. The distances of these positions were 75ft, 100ft, and 150ft far from flare flame as shown in Figure 4. The thermal radiation from single tip burner obtained at different position and wind speed are included in Table 1.

Three tip burner utilized ethylene as a flaring gas to measure heat radiation from flare flame in three different locations with wind blowing from south to the north direction. The set up for taking measurements is shown in Figure 5. Heat radiation from three tips burner flare system results for the different position and 11.2mph for cross wind speed are summarized in Table 2. Three varies burner pressure were implemented with two burner sizes to measure heat radiation from flare flame. These measurements were taken at two different positions, 15m and 30m from flare flame as shown in the test setup which depicted in Figure 5.

Table 2: Measured thermal radiation flux for 3-tips flare.

Tip Size (inch)	Location (m)	Burner Pressure (psi)	Thermal Radiation Measurements (W/m ²)
3	15	2.8	3344
3	15	7.3	4803
3	15	11.4	6192
3	30	2.8	671
3	30	7.3	1184
3	30	11.4	1532
4	15	2.8	6371
4	15	7.3	8192
4	15	11.4	9536
4	30	2.8	1513
4	30	7.3	2464
4	30	11.4	2747

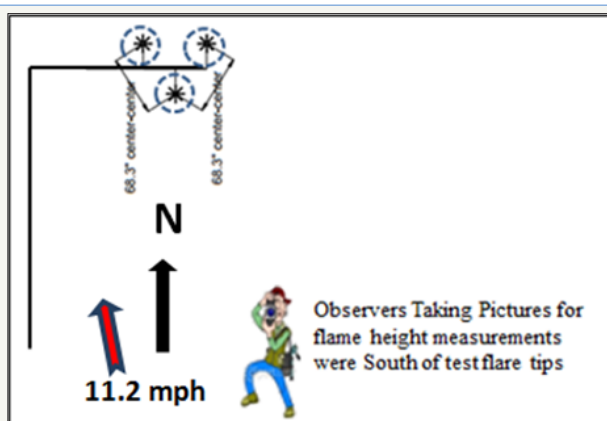
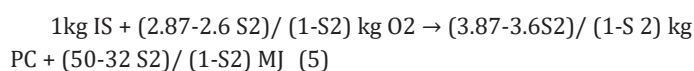
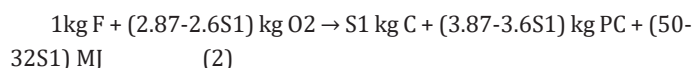


Figure 5: Setup for radiation measurements from three tips flare.

Reaction mechanism

Numerous reaction mechanisms have been suggested to conduct a detailed kinetic modelling of combustion reaction that has ability to solve the combustion chemistry and predict concentrations of reaction components. Among these mechanisms, Smith et al. [15,19] suggest simplified four step chemical reaction mechanism to approximate the flare gas combustion.



Previous validation work has been carried out to assess the accuracy of the combustion scheme shown above which has also been incorporated into a CFD based flare model [14] applied to several gas flare systems. The first reaction represents hydrocarbon fuel combustion and describes the incomplete reaction of Fuel (F) with oxygen (O_2) to produce Products of Combustion (PC) and black carbon (C) and some energy (MJ). This reaction produces S1 kilograms of black carbon per kilogram of fuel consumed where S1 depends on the fuel type (0.005 used for light hydrocarbons [20]). The second reaction represents the endothermic fuel pyrolysis or cracking reaction which produces S2 kilograms of black carbon (0.15 used for light hydrocarbons) and Intermediate Species (IS) such as carbon monoxide. The third reaction consumes black carbon and more oxygen to produce carbon dioxide (CO_2) and

some energy. The final reaction consumes the Intermediate Species formed in the second reaction plus some additional oxygen to form combustion products and energy.

CFD modeling

Three computations for single tip, three tips, and multi-tip flares were conducted using C3D software. The turbulent reaction chemistry coupled with radiative transport between buoyancy driven fires and surrounding objects was simulated using this tool.

Physical parameters: For the purposes of modeling of this study, an average gas density of 1.04kg/m^3 was assumed. Also, a standard gas pressure and temperature of 1atm and 293.15K was used. Moreover, an average molecular weight of 25kg/kmol for the volume flow for each flare was considered in the available operating data.

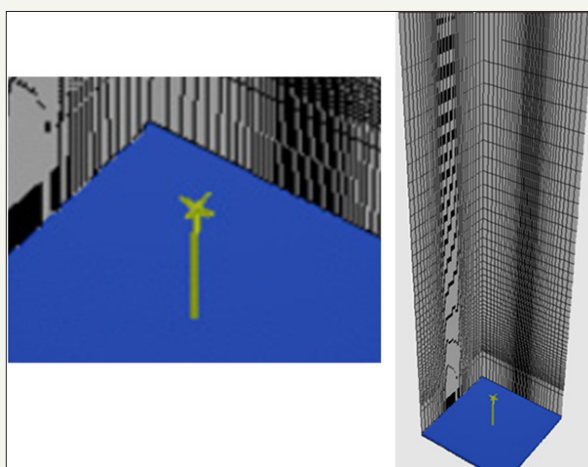


Figure 6: single Tip flares mesh [13].

Single tip flare modeling: To obtain the flame dynamics as flame shape and size of single flare tip, CFD simulation cases have been performed. Also, thermal radiation and soot estimation were found using these computations. The simulations was carried out using 3-D physical domain with dimensions of 6m, 6m, and 26m

for the length, width, and height respectively. The flare tip was located 2m above the ground level. Rectangular cells were used to construct the mash of physical domain where the number of cells in this domain was 110,000 cells as shown in Figure 6.

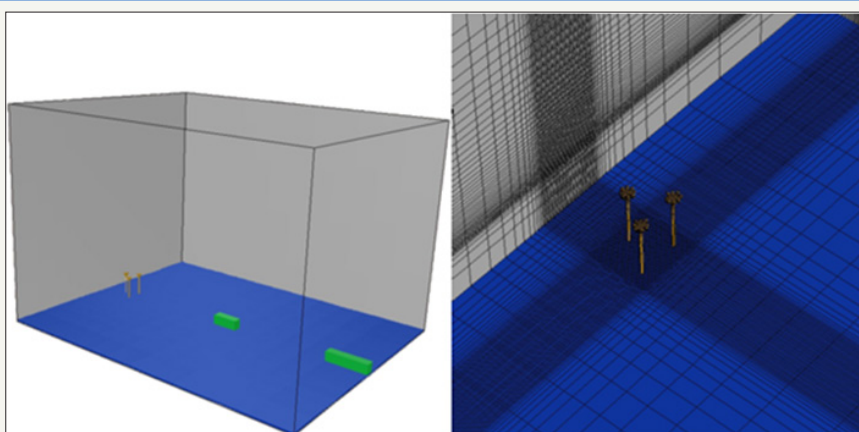


Figure 7: Geometry and Mesh for 3-tips Flare [13].

Three tip flare: The 3-D domain of 30, 35, 25m dimensions was used for simulation with radiation meters (solid boxes) which distance in 15m and 50m respectively from the flare burners for the three tips flare as shown in Figure 2. The mesh was refined locally

near burner tips and radiation measuring unit. The total number of control volumes was 188,000 of computational cells as shown in Figure 7.

Multi tips flare system: There are many issues that associated with multi tip flare system design. One of these issues is included the difficulties of anticipated flare gas flow rates and flaring duration. Also, feed composition and its temperature conditions to flaring system is complex to specify. Moreover, flame height with

respect to the fence height should be considered in the design task. Furthermore, noise and radiation to the surrounding are critical to the design process. For multi-tip flares, a very large composite plume is created from plumes from each individual flare burner merging into one as shown in Figure 8.

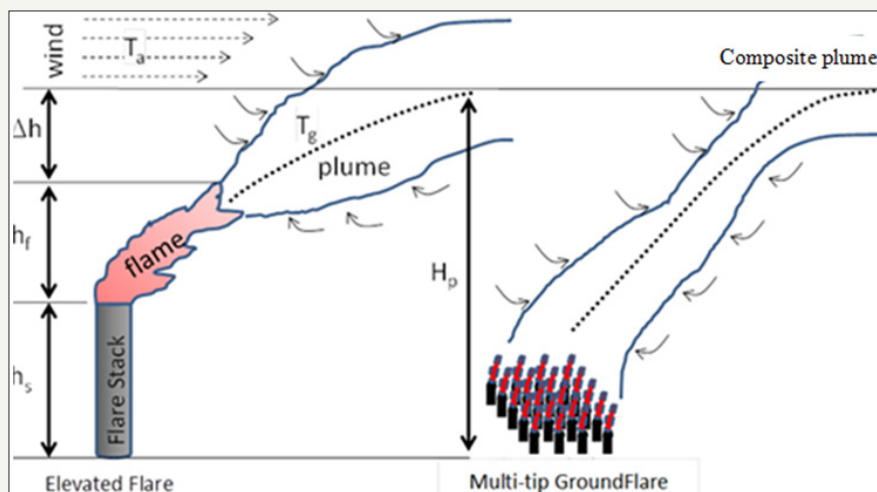


Figure 8: Multi tip flare plume formation [21].

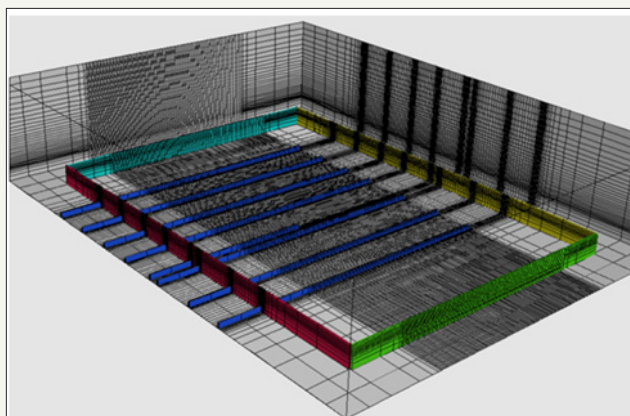


Figure 9: Multi-tip flare field mesh [13].

Due to the large field of this kind of flare system, large flare plume formed, and the risk associated with high flame temperature and heat radiation, the flare performance quantification is difficult to perform. Therefore, simulations with suitable simulation package are used to quantify flare performance with different scenarios. Around the full multi-tip flare field wind fence. The main objectives of this fence are to protect workers and equipment from thermal radiation and to protect flame shape from high wind speed that could affect the flame shape or may cause flame extinguishment. An understanding of flare tip performance and wind effects on flame are required in order to estimate emissions from MTF. Also, more understanding with respect to the effects of the wind and tip geometry on flame are needed. Also, knowledge the analysis of the transient flame, near tip mixing for hundreds of tips in large flare fields is wanted. To integrate these effects together, CFD modelling are used to simulate these systems efficiently. The multi-tip flare field domain size was 35, 35, and 25 meters for the length, width, and height respectively. Figure 9 presents the mesh of multi tip flare

system that included 1.2 million cells in which local refinement near burner rows and tips was applied. To reduce computational time cost, rectangular orthogonal cells were used in all simulation cases. Two speeds for wind which are zero and 7mph were considered for all simulations. Also, propane and ethylene gases were used as flare vent gases. The CFD model that validated against single and three tips flare experimental data was used to simulate multi tip flare performance.

CFD Fundamental Models

C₃d tool of CFD technique was used to obtain numerical solutions for a 3D flare domain by simulating single tip and three tips flare performance. Large Eddy Simulation (LES) as the turbulence model was used. The governing equations for the LES model assuming incompressible fluid flow are given below [22]:

The continuity equation is given in equation 6:

$$\partial(\rho u_i) / \partial x_j = 0 \quad (6)$$

where “ ρ ” is the gas density and “ u_i ” is the gas velocity vector.

The momentum equation is shown in equation 7:

$$\partial(\rho u_i u_j) / \partial x_j = \partial P / \partial X_i + \partial \tau_{ij} / \partial X_j + \rho f_i \quad (7)$$

With f_i as the body forces, P as the pressure, and τ_{ij} represented as the stress defined in equation 8:

$$\tau_{ij} = \mu(\partial u_i / \partial x_j + \partial u_j / \partial x_i) + (\mu_B - 2/3\mu)\partial u_k / \partial x_k \delta_{ij} \quad (8)$$

The other governing equation to be solved is the energy equation (equation 10). The C3d form of this equation is introduced below:

$$\rho c_{p0}(T) / \partial x_j = -(\nabla \cdot q) - (\frac{\partial \ln \rho}{\partial \ln T} \frac{Dp}{Dt} - (\tau : \nabla v)) \quad (9)$$

Where C_p is the specific heat

To resolve sub-filter scales for LES turbulence model, the Gaussian filter is used as shown in equation:

$$G(X-r) = [(6/(\pi\Delta^2))]^{1/2} \exp(-(6(X-r)^2/\Delta^2)) \quad (10)$$

The following equations are used to model the kinetic energy dissipation on sub grid scales to molecular diffusion is present in equations (11) and (12):

$$\tau_{ij}^r - 1/3\tau_{kk}\delta_{ij} = -2\nu_t\bar{S}_{ij} \quad (11)$$

$$\bar{S}_{ij} = 1/2(\frac{\partial \bar{u}_j}{\partial X_i} + \frac{\partial \bar{u}_i}{\partial X_j}) \quad (12)$$

with τ_{ij}^r as the stress tensor, \bar{S}_{ij} as the rate-of-strain tensor, and ν_t as the turbulent eddy viscosity.

The eddy viscosity is approximated as the characteristic length scale times the velocity scale in most subgrid scale models as illustrated by the Smagorinsky-Lilly model:

$$\nu_t = (C_s\Delta_g)^2 \sqrt{2\bar{S}_{ij}\bar{S}_{ij}} = ((C_s\Delta_g)^2 |S|, C_s = \text{Constan } t, \Delta_g = \text{gridsize}) \quad (13)$$

Single tip and three tips flares

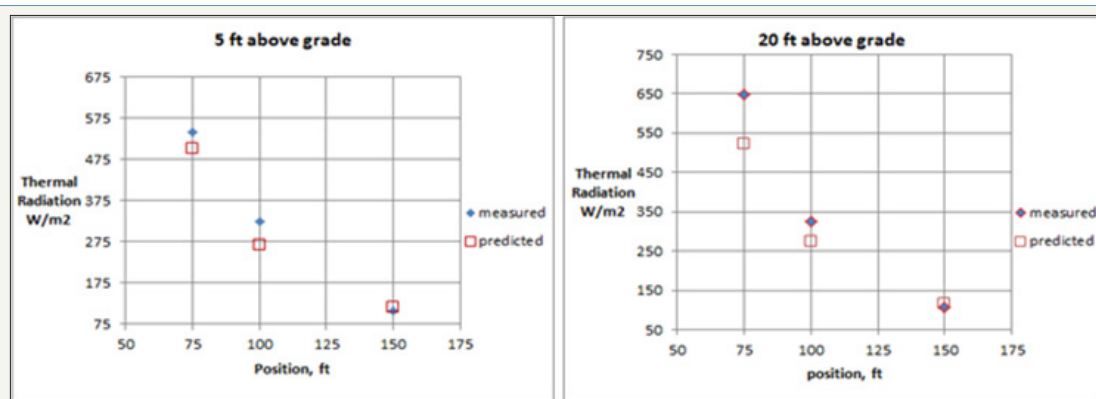


Figure 10: Comparison of predicted and measured thermal radiation for single tip flare (wind speed = 12mph).

Figure 10 & Figure 11 show comparisons between experimentally measured thermal radiation with that predicted by a C_3d simulation with a wind speed of 12 and 6mph respectively. Figure 11 shows very good agreement between experimental and predicted thermal radiation from single tip flare with wind speed of 6mph. The predicted data for a 12mph wind tends to

The equilibrium assumption was applied between energy production and dissipation of small scales in this model. The multi species conversation equations form is shown in equation (14)

$$\frac{\partial \rho m_i}{\partial t} + \nabla \cdot \rho V m_i = -\nabla \cdot J_i + R_i + S_i \quad (14)$$

Where, m_i is the mass fraction of species i , J_i diffusion flux of species i , R_i is the mass creation or depletion by chemical reactions, and S_i source of mass.

Results and Discussions

Annual flare emissions

During the ignition process, flare gas fed to the atmosphere has insufficient momentum and time to completely mix with sufficient oxygen to fully burn the flare gas which results in excessive black carbon (soot) formation during the pyrolysis step (reaction 2 of the 4- step mechanism shown above). Nearly all flares exhibit the characteristic black smoke puff (un-reacted black carbon or soot) formed by incomplete combustion which occurs during the transient ignition process. Practical experience with gas flaring suggests the transient ignition process lasts approximately 10 to 30 seconds before sufficient oxygen is entrained into the flame to completely burn the black carbon (smokeless operation). A conservative estimate for combustion efficiency during the ignition process is between 50 and 75%. Given the number of flare ignition events per year and assuming an average gas density and molecular weight derived from flare operating data, an estimate of un-reacted hydrocarbon emissions from these flares can be approximated. As an example, consider that Iraq flared around 17,730 million cubic meters of waste gases in 2016 [2]. Assuming an average weekly operating time for a standard gas flare of 5 hours per week, the amount of flare emissions released from Iraqi flares would range between 2,563,037 and 5,126,097 kg/year (depending on combustion efficiency during the ignition phase).

be underestimated compared to the experimental data which may be due to the unsteady nature of higher wind speeds and its impact on flame shape hence causing the radiation flux to have a larger variance. For the same position with varying wind velocity, the thermal radiation decreases with increasing wind speed (see Figure 10 & Figure 11). This is most likely caused by shorter flames

produced by increased mixing rate thus lowering the effective amount of radiating soot in the flame. A secondary effect may also be higher wind velocities increase the cooling rate for the flame

which reduces the flame temperature and associated radiative flux from the flame and the radiometer.

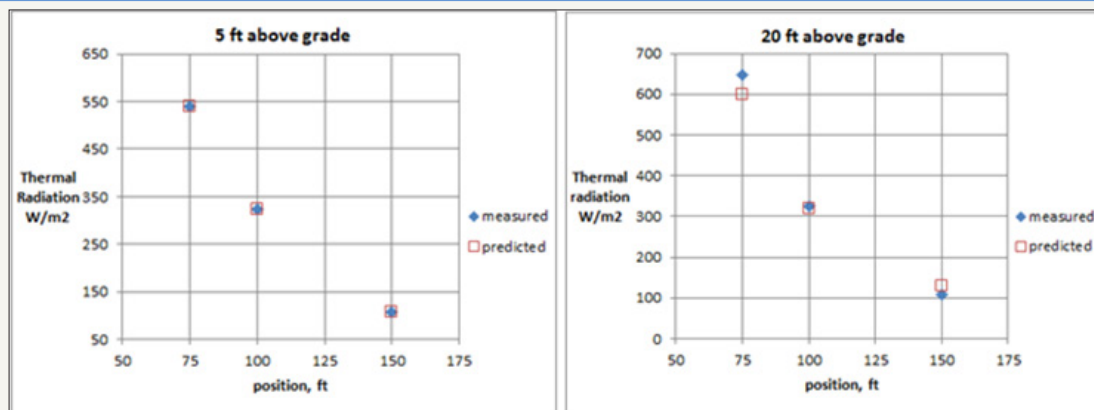


Figure 11: Comparison of predicted and measured thermal radiation for single tip flare (wind speed = 6mph).

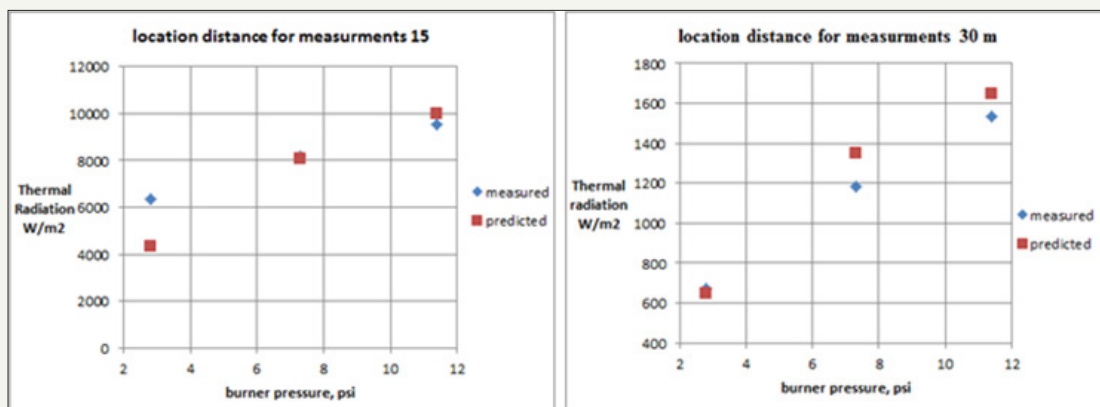


Figure 12: Comparison of predicted and measured thermal radiation for three tips flare (tip size=4).

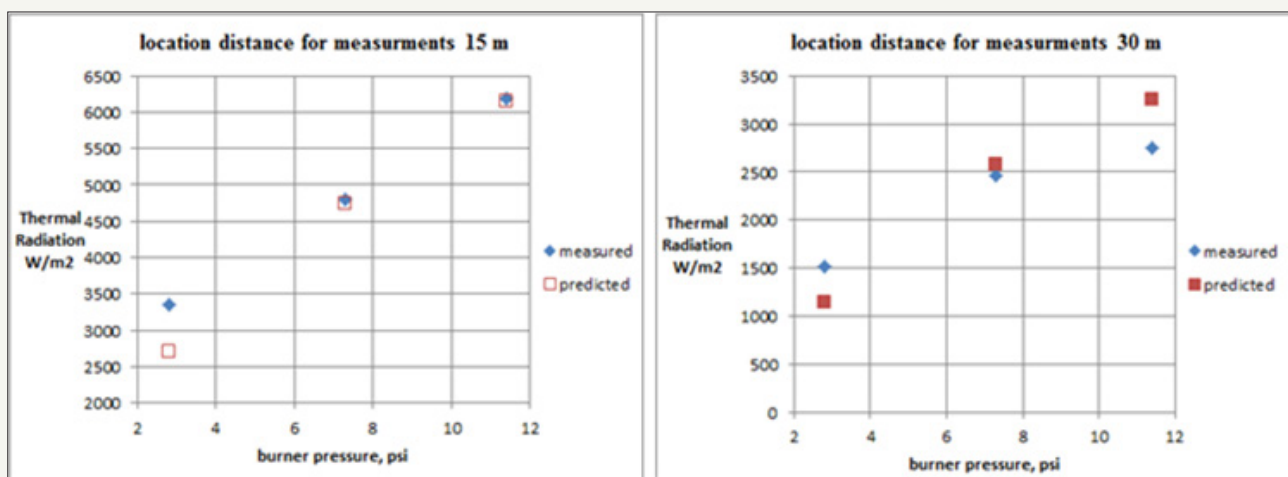


Figure 13: Comparison of predicted and measured thermal radiation for single tip flare (tip size=3).

The measured and predicted radiation data for three flare tips are shown in Figure 12 & Figure 13 with two tips sizes, operating with varying tip pressure. Results indicate an increase in thermal radiation with increasing burner pressure. This is likely due to a larger flame created by higher flare gas flow associated with higher tip pressure. Figure 12 & Figure 13 shows good agreement between experimental and predicted data for thermal radiation.

Thermal radiation emission

The effect of wind speed on the heat radiation at burner pressure of 2.8psi and at distance of 50 foot is shown in Figure 14. This figure indicates decrease in the thermal radiation with increasing the wind velocity. This decreasing could be a result of the reducing of flame temperature with high wind velocity.

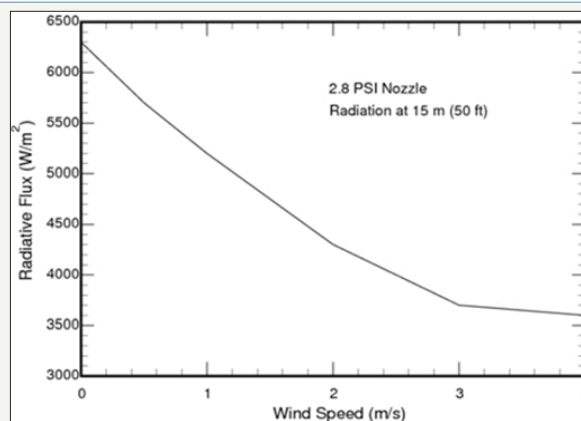


Figure 14: Impact of wind speed on thermal radiation flux [14].

Multi tips flare system

The predicted flame height and heat radiation for full field of 405 burner tips is presented in Figure 15. Also, the combustion products are shown in the same figure. The heat radiation rate

was found to be 61000 and 35000 watt/m² on the left and right walls respectively for the peak flow of flue gases. Moreover, values of 6600 and 6600 watt/m² on the left and right walls respectively, when the flow is sustainable, are obtained for the heat radiation. These cases were performed with no wind effect.

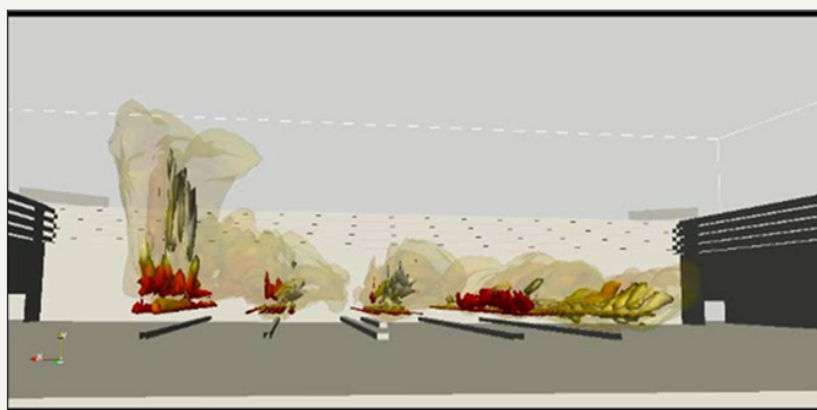


Figure 15: Flame size, shape and combustion products prediction for MTF system [13].

Conclusion

Testing has been conducted for a single flare tip and a 3-flare tip system to measure the flame height and radiation flux when burning propane and Tulsa natural gas. These tests were conducted in a no-wind ambient condition as well as a 6-12 mile per hour wind conditions. The non-wind flame height for the single flare tip test was measured to be 48-53ft high while the flame height in windy conditions was measured to be approximately 35ft high. In the windy condition, the flame was also wider and had less radiation flux than the flame in non-wind conditions. The multi-tip tests were conducted to assess flame interaction and cross lighting of adjacent flare tip burners using a single pilot. The three tip tests showed a flame height essentially the same as the single flare tip test. This indicated the flames operated independently and did not merge into a single larger/taller flame. Testing showed that as the tip pressure increased from 2.8psi to 11.4psi the flame height increased as did the radiant flux (3344 W/m² to 6192 W/m²). This same behavior was observed for the larger 4" flare tip.

Given the test results, a detailed CFD model was developed and used to simulate the flare flame shape and height for various flare

gas flow rates, tip pressure and size and ambient wind conditions. Predicted soot levels and radiant heat flux from the single and multiple flare tests were compared to the measured values to validate the model. Using the validated model, predictions for single, three, and multi tip flare systems were performed using an LES based CFD model. The validated CFD model was also used to simulate a large industrial multi-point ground flare system burning approximately 260kg/s of flare gas. Using the validated flare model, the predicted radiation from a single and three flare tip showed good agreement with the measured data. In addition, simulation of a 400 multi-tip ground flare system provided a reasonable estimate of the flame shape and flame height with the associated heat radiation profile on the surrounding wind fence and nearby equipment. Furthermore, at the maximum possible flare gas flow and at the sustained flare gas flow, the heat radiation predicted on the wind fence walls were estimated. Finally, annual flare emissions created during the transient ignition phase of flare operation have been estimated assuming an average flare gas molecular weight and density plus an average ignition time and conservative combustion efficiency during the ignition phase. Based on these assumptions, we have estimated flare emissions for Iraq to be between 2,563,037

and 5,126,097 kg/year. These estimates illustrate the impact open flaring may have on the environment. They also demonstrate the need for advanced sensor technology to reliably measure flare performance. Using advanced sensor technology promises to allow plant operators to better control flare emissions and find ways to reduce the environmental impact of gas flares.

References

1. Elvidge CD, Zhizhin M, Baugh K, Hsu FC, Ghosh T (2016) Methods for global survey of natural gas flaring from visible infrared imaging radiometer suite data. *Energies* 9(14).
2. <http://www.worldbank.org/en/programs/gasflaringreduction#7>.
3. Enforcement Alert (2012) EPA enforcement targets flaring efficiency violations. *Enforcement Alert* 10(5).
4. API Standard 521 (2012) Guide for pressure-relieving and depressuring systems. American Petroleum Institute.
5. US EPA (2009) Integrated science assessment (ISA) for particulate matter (Final Report, Dec 2009). US Environmental Protection Agency.
6. Conrad BM, Johnson MR (2017) Field measurements of black carbon yields from gas flaring. *Environ Sci Technol* 51(3): 1893–1900.
7. Johnson MR, Devillers RW, Thomson KA (2013) A generalized SKY-LOSA method to quantify soot/ black carbon emission rates in atmospheric plumes of gas flares. *Aerosol Science and Technology* 47(9): 1017-1029.
8. McEwen JD, Johnson MR (2012) Black carbon particulate matter emission factors for buoyancy-driven associated gas flares. *J Air Waste Manag Assoc* 62(3): 307-321.
9. Allen DT, Smith D, Torres VM, Saldana FC (2016) Carbon dioxide, methane and black carbon emissions from upstream oil and gas flaring in the United States. *Current Opinion in Chemical Engineering* 13: 119-123.
10. Lack DA, Moosmüller H, McMeeking GR, Chakrabarty RK, Baumgardner D (2014) Characterizing elemental, equivalent black, and refractory black carbon aerosol particles: a review of techniques, their limitations and uncertainties. *Anal Bioanal Chem* 406(1): 99-122.
11. Weyant CL, Shepson PB, Subramanian R, Cambaliza MOL, Heimbürger A, et al. (2016) Black carbon emissions from associated natural gas flaring. *Environ Sci Technol* 50(4): 2075-2081.
12. Wang A, Lou HH, Chen D, Yu A, Dang W, et al. (2016) Combustion mechanism development and CFD simulation for the prediction of soot emission during flaring. *Front Chem Sci Eng* 10(4): 459-471.
13. Smith JD, Jackson R, Suo-Antilla A, Smith S, Allen D (2014) Achieving environmental compliance through proper destruction efficiency of low-profile multi-tip flare systems. American Flame Research Committees.
14. Smith J, Suo Antilla A, Smith S, Modi J (2007) Evaluation of the air-demand, flame height, and radiation load on the wind fence of a low profile flare using ISIS-3D. AFRC-JFRC.
15. Smith J, Suo Antilla A, Philpott N, Smith S (2010) Prediction and Measurement of Multi-Tip Flare Ignition. American Flame Research Committees-International Pacific Rim Combustion Symposium, Advances in Combustion Technology: Improving the Environment and Energy Efficiency.
16. Smith J, Jackson R, Suo-Anttila A, Hefley K, Wade D, et al. (2013) Prediction and measurement of multi-tip flare ignition. American Flame Research Committees.
17. Smith J, Jackson R, Suo-Anttila A, Hefley K, Smith Z, et al. (2015) Radiation effects on surrounding structures from multi-point ground flares. AFRC 2015 Industrial Combustion Symposium.
18. Miller D (2017) New model for predicting thermal radiation from flares and high pressure jet fires for hydrogen and syngas. *Process Safety Progress* 36(3): 237-251.
19. Smith J, Jackson R, Sreedharan V, Suo Anttila A, Allen D, et al. (2016) Withstanding the wind. *Hydrocarbon Engineering* 21(10): 43-49.
20. Said R, Garo A, Borghi R (1997) Soot Formation Modeling for Turbulent Flames. *Combustion and Flame* 108(1-2): 71-86.
21. Smith JD, Suo Anti A, Jackson R, Smith S (2012) Prediction of Plume Formation and Dispersion from Gas Flares. American Flame Research Committee Meeting, Salt Lake City, Utah, USA.
22. Smith J, Adams B, Jackson R, Suo Anttila A (2017) Use of RANS vs LES modelling for industrial gas-fired combustion. *Industrial Combustion*.



Creative Commons Attribution 4.0 International License

For possible submissions Click Here

[Submit Article](#)



Progress in Petrochemical Science

Benefits of Publishing with us

- High-level peer review and editorial services
- Freely accessible online immediately upon publication
- Authors retain the copyright to their work
- Licensing it under a Creative Commons license
- Visibility through different online platforms